

# Assessment of the Symmetry and Deformation of a Submarine Hull Using the PCSE Method

Paweł Dąbrowski\* 

Department of Geodesy, Gdańsk University of Technology, Gdańsk, Poland

Łukasz Marchel 

Polish Naval Academy; Department of Navigation and Maritime Hydrography, Gdynia, Poland

Radosław Kiciński 

Polish Naval Academy; Department of Navigation and Maritime Hydrography, Gdynia, Poland

Roderik Lindenberg

Delft University of Technology; Department of Geoscience and Remote Sensing, The Netherlands, Netherlands

\* Corresponding author: [pawel.dabrowski1@pg.edu.pl](mailto:pawel.dabrowski1@pg.edu.pl) (Paweł Dąbrowski)

## ABSTRACT

*The paper presents a new dry-dock method for assessing the deformation of submarine hulls using TLS point cloud data and the point cloud spatial expansion method (PCSE). The advantage of the proposed approach is the high-resolution deformation analysis that can be conducted in the case of both the availability and a lack of technical documentation on the submarine hull. The geometry assessment involves two-plane hull symmetry in longitudinal sections of a tested Kobben-class submarine located in Gdynia, Poland. The features of PCSE introduce additional geometrical parameters that are not available in the original point cloud method. The procedure for local fitting of a plane into the expansion eliminates the problem of varying densities of the hull point cloud. Accuracies of several millimetres are achieved and are applicable to multi-temporal monitoring of the deformations of submarine hulls. The assessment of similar deformations is not possible in the original point cloud method, due to the unknown parameters of the orientation and curvature of the convex cylindrical hull surface. The PCSE-based parameterisation presented here enables the creation of alternative quasi-planar point cloud projections to extract new spatial information on the object. The results of this study were verified using theoretical values derived from design data on the Kobben-class submarine, and demonstrated the effectiveness of our method in terms of detecting deformations even without design references. The proposed methodology is uniform, and can be adapted to other symmetrical structures.*

**Keywords:** Hull deformations, Symmetry, Spatial expansion, Laser scanning, PCSE

## INTRODUCTION

The detection of hull deformation is crucial in order to maintain the structural integrity and safety of submarine vessels. The technical state of the hull is traditionally assessed during docking periods of the vessel, and visual inspection is used to detect signs of deformation such as bulges, cracks, or dents. Other non-destructive methods used in the assessment process include finite element analysis (FEA) [1], magnetic particle inspection (MPI) [2], eddy current testing (ECT) [3] and ultrasonic testing (UT) [4]. In some cases, strain gauge

sensors are used to measure the deformation or strain of the submarine hull [5]. A digital representation of the hull's surface can be obtained using laser scanning technology; in this case, point clouds can be compared with the design specifications to identify deviations or deformations of the tested object. The nature of the deformation, accessibility to the affected areas, and the accuracy requirements determine the selection of an appropriate method of assessing the hull shape.

Submarine hull deformations are described by a set of geometrical, structural, and physical parameters that

determine whether further actions are needed for maintenance or repair of the vessel. Displacements in the hull structure, such as bulges and buckles, dents, or distortions [6], refer to changes in the position or shape of the hull from its original form, while deflection [7] refers to bending or flexing due to loading conditions or external forces. The locations of cracks and fractures [8] indicate structural weaknesses and potential points of failure in the submarine hull. Degradation of the metal surface, caused by corrosion and pitting [9], indicates parts of the hull that represent potential weak spots in terms of deterioration. Both hydrostatic testing [10] and hull stress testing [11] are used to evaluate hull leaks or deformations. The parameters are interrelated, and a comprehensive assessment considers multiple factors when evaluating the overall condition of the submarine hull.

The symmetry of the ship's hull is an additional factor that extends the scope of spatial analyses. Currently, one of the most accurate methods of mapping and parameterising spatial objects is laser scanning [12]. Terrestrial laser scanning (TLS) enables highly accurate and detailed measurements by capturing millions of individual points representing the 3D geometry of the scanned area [13]. The advantages of this technology include rapid data collection with accuracies of up to the millimetre level, low cost compared with traditional manual measurements, accessibility of irregular and hard-to-reach surfaces, and a permanent record of the scanned environment, enabling multi-temporal analyses. Advanced point cloud registration algorithms [14] are available to align multiple scans into a single common point cloud that can enable full digitisation of complex objects without major reductions in accuracy.

However, point clouds do require additional processing before the desired spatial information can be extracted to achieve the goal of submarine hull shape assessment. Leaving aside the basic registration procedure, in which multiple separate scans are aligned and merged into a single unified point cloud [15], several approaches can be used to create useful output. Segmentation of a point cloud involves dividing it into meaningful segments based on specific criteria or object features, such as smoothness, orientation or intensity [16]. Machine learning (ML) techniques can be applied to recognise, classify, and label objects within the point cloud based on dictionaries of classes or categories [17]. Surface reconstruction is used in urban-area point clouds to create continuous 3D models from discrete point clouds [18], which are later used in mesh-based rendering and visualisation [19]. For non-robust methods, obtaining acceptable results requires the removal of statistical outliers or the application of voxel-based filtering to enhance the quality of the dataset [20].

During immersion, the hull of a submarine is subjected to water pressure on all sides, which increases with depth. This pressure acting on the hull causes it to undergo elastic deformation, reducing its volume and resulting in a loss of buoyancy. The change in buoyancy can be determined by calculation or practical testing. In order to calculate negative buoyancy, it is necessary to know the value of the volumetric hull compression coefficient, which depends on the working

depth and the displacement of the submarine. Ships and vessels are assessed in terms of hull operation based on thickness measurements and possible post-collision and wave deformations. Professional controllers from classification societies such as the Polish Register of Shipping, Lloyd's Register of Shipping, DNV GL, and Bureau Veritas assess the condition of the hull based on their own experience and the association's internal guidelines, although unfortunately, the numerical values used in these classifications are not public information. In this study, we intentionally chose the hull of a decommissioned submarine to illustrate the possibilities of using the proposed method. After long-term operation, the ship has many deformations that are often invisible to the naked eye, and may be seen when the hull is compared to the technical documentation.

For a Kobben-class submarine, permanent plastic deformations may appear after exceeding a depth of immersion of 225 m, which can be detected during testing using 3D measuring instruments (such as a tacheometer, tracker, or laser scanner). According to the technical documentation, changes in the hull diameter in the elastic range can reach 6 mm, and such a small change may be overlooked during shipyard measurements. The proposed method is an extension of standard methods, with additional imaging of the ship plating condition. Moreover, observation of the hull of the ship in this case showed that it was not properly supported, which is why it was deformed due to gravity in the bow area. Plating therefore had to be developed around the neutral axis of the hull, as determined based on the technical documentation. This approach is more effective for ship hulls that have been deformed as a whole (e.g. after collision or breaking mooring lines and hitting the quay), because standard measurement methods do not include measurements along the neutral axis and may miss the deformation of the hull as a whole due to local deformations.

The main aim of this paper is to present a new dry-dock method for assessing hull deformation on a larger scale than is possible with classical measurement methods, such as tachymetric measurements. The test object was a Kobben-class submarine located in Gdynia, Poland. Cracks, bends, and other shape anomalies can cause significant damage to the hull, and affect the combat operations of submarines at great depths under high water pressure. The proposed method significantly broadens the spectrum of hull deformation analyses, and eliminates the factor of variable point cloud density by exploiting the properties of the point cloud spatial expansion (PCSE) method. The innovative aspect of this study is the possibility of assessing the deformation of the hull regardless of the availability of technical documentation, through consideration of the symmetry of both boardsides of the vessel. The assessment was validated by comparing the actual hull shape with technical documentation for the vessel. The analyses conducted here showed differences of several millimetres in deformation, both with and without of the availability of project data, meaning that that the proposed solution is effective in both cases. The methodology presented here also enables the assessment of hull bends

and deformations not only of submarines but also of civil ships, warships, and parts of airplanes. In addition, the steps involving axis estimation and point cloud transformation enable effective comparison of hull shape changes and monitoring of the trends in these changes when performing regular periodic measurements using laser scanning technology.

## MATERIAL AND METHODS

### TLS MEASUREMENTS AND POINT CLOUD REGISTRATION

The test object assessed here is a Kobben-class submarine, a diesel-electric submarine that was developed by the Norwegian Navy in the late 1950s and early 1960s. The overall length of the vessel is approximately 46 m, and it generally has a submerged displacement of around 400 tons, although the tested submarine had 572 tons of underwater displacement. The hull is constructed using high-strength steel alloys. Kobben submarines operate on a diesel-electric propulsion system: diesel engines drive generators that produce electricity to power the electric motors driving the propellers. Kobben-class submarines were equipped with eight 533 mm torpedo tubes in the bow section and sonar systems for detecting and tracking underwater targets, and the crew consisted of approximately 25 personnel. These submarines were primarily designed for coastal defense and anti-submarine warfare operations [1]. The submarine considered in this study was located at the Polish Naval Academy of the Heroes of Westerplatte in Gdynia, Poland, and is shown in Fig. 1.



Fig. 1. Point cloud for a Kobben-class submarine (left panel) as measured by a Leica ScanStation P50 laser scanner (right panel)

Eight laser scanner stations were set up to acquire a digital model of the hull, and scans were registered with an RMS error of 1.2 mm. The Kobben-class submarine in Gdynia has two entrances cut into the port side (shown to the right

of Fig. 1), and those parts of the hull were therefore excluded from the analysis. The submarine point cloud consisted of 97 million points, with a mean surface density of 8 mm, and did not represent the keel. Due to limited access, the resolution of the points on the deck at the front of the submarine was lower compared to the other parts of the ship. The factors mentioned here represent limitations of this study in terms of the analysed source data.

### PRE-PROCESSING OF THE POINT CLOUD

The assessment of hull deformation required preliminary processing of the point cloud, which involved the features of the PCSE method. The PCSE method enables the representation of a symmetrical object in an alternative form. The expansion modifies the structure of the point cloud by projecting 3D coordinates, thus enabling the examination of points as a quasi-planar model with the attribute of height. As a result, additional geometric parameters related to the object's symmetry axis can be obtained that are not directly available in the original point cloud. The PCSE method can be used for various types of symmetrical objects, including cylindrical [21] and prismatic [22] shapes. Previous work on this method has focused on assessing the structure, shape, and deformation of buildings; however, the universality of this approach allows it to be used on other engineering structures such as submarine hulls.

Data pre-processing was performed in several steps. The first step involved the selection of coordinates of characteristic points representing the position of the submarine hull in the global coordinate system of the registered point cloud. Next, vector calculations were introduced to define the course of slightly inclined horizontal and vertical planes

that coincided with the gathered points. After these calculations, the rotation angles were determined and used for an initial coarse alignment of the hull point cloud along the X-axis. In the next step, narrow orthogonal cross-sections were selected, and their centers were determined using robust estimation. The set of cross-section centers was then used to fit a line in three-dimensional Euclidean space using the total least-squares method. In the final step, the parameters of the estimated

submarine axis were used to perform the final set of elementary rotations to bring the point cloud into alignment with both the submarine and the X-axis. This condition is obligatory in order to obtain a PCSE expansion of the hull representing the spatial relations between the points and the submarine axis.



An important element when using the PCSE method involves determining the axis of symmetry of a symmetrical object. In the case of engineering objects with unknown deformations, axis estimation is based on narrow cross-sections of the point cloud. Both non-robust and robust estimation methods were used to determine the course of the axis along the geometric centers of cross-sections at fixed heights of the object [23]. The set of cross-section centres is a discrete representation of the axis of a symmetrical object, based on which a 3D line representing the axis of symmetry is estimated [24]. The coordinates of the vector of this axis enable verticalisation of the point cloud for highly slanted objects and a spatial expansion taking into account the course of the object's axis [22].

The application of the PCSE method to assess the symmetry and deformation of a submarine required modifications to the original projection formulas. The required transformation was determined from the parameters of the axis of symmetry of the submarine. Taking into account an undefined orientation of the TLS point cloud of the Kobben submarine, the course of the axis was estimated by a two-stage transformation. The initial transformation provided a coarse fitting of the hull to the X-axis (Fig. 2). The transformation parameters were determined based on two points on the keel axis ( $P_A$  and  $P_B$ ) and one point located in the symmetrical plane of the ship's sail ( $P_C$ ). Points  $P_A$  and  $P_B$  were estimated as local central points in the two opposite parts of the keel at the front and back of the submarine. In this operation, the point cloud cross-sections were used to represent the two sides of the keel measured by the laser scanner, and two points were then determined in the middle of the keel at the bottom. The third point  $P_C$  is located at the local extreme of curvature of the back side of the submarine sail.

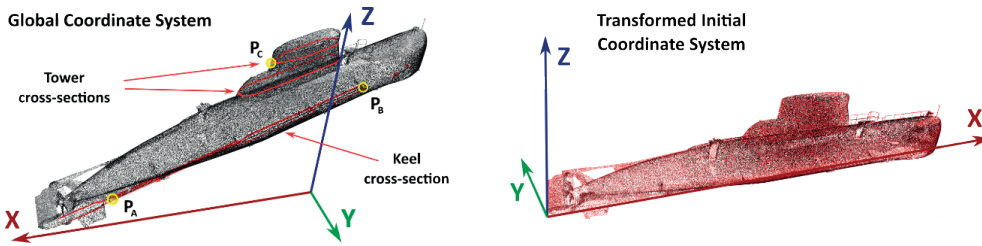


Fig. 2. Initial transformation of the submarine point cloud resulting in the front-back directional alignment

The vectors  $U = P_B - P_A$  and  $V = P_C - P_A$  determine the vertical plane of symmetry containing the ship's structural axis. The vector  $U$  runs along the keel axis, while  $V$  runs in the diagonal direction between a point on the keel and the perimeter plane of the sail. The vector orthogonal to the plane was determined from the relationship:

$$W = V \times U \quad (1)$$

The origin of the coordinate system for the transformed point cloud was located at the rear edge of the ship's rudder

blade. Using the vector equation for a straight line, the value of the parameter was calculated, which determined the starting point of the system and the corresponding point located on the edge of the rudder blade:

$$P_0 = P_A + t_0 U \quad (2)$$

where  $t_0 = (x_V(x_{P_A} - x_Q) + y_V(y_{P_A} - y_Q) + z_V(z_{P_A} - z_Q)) / |U|^2$ .

Next, two elements of the transformation of the registered point cloud of the submarine were determined (left panel of Fig. 2). The first stage of the transformation involved the translation of points from the cloud by the vector  $T_0 = -P_0$ , and the second stage involved a rotation defined by the  $R_0$  matrix:

$$R_0 = ([u \ v \ w]^T)^{-1} \quad (3)$$

where  $u, v, w$  are the unit vectors of the subsequent vectors  $U, V \times W$  and  $W$ . The vector product  $V \times W$  determines the vector located in the symmetrical plane of the ship while maintaining the condition of orthogonality to the two vectors  $U$  and  $W$ . Thus, the vector  $v$  replaces the vector  $V$  used in Eq. (1). The initial point cloud transformation formula shown in the right panel of Fig. 2 finally takes the form:

$$P' = R_0(P + T_0) \quad (4)$$

where  $P$  is the vector of point coordinates from the registered cloud  $[x_P \ y_P \ z_P]^T$ .

This initial transformation ensured that the point cloud complied with the conditions of parallelism of the keel with the X-axis and verticality of the ship's symmetry plane with the accuracy of fitting the keel axial points  $P_A$  and  $P_B$ , and the point  $P_C$  on the ship's sail (cf. left panel of Fig. 2).

Next, the submarine axis in the transformed submarine point cloud was determined, and a set of 1.5 mm wide cross-sections of the ship's hull was extracted (left panel of Fig. 3). In each section, filtration was performed to eliminate outliers that did not belong to the cylindrical surface of the hull (right panel of Fig. 3). Then, using least squares, the centres of the cross-sections were determined, which represented the final estimation of the hull axis.

The centres of the cross-sections are a discrete representation of the axis of symmetry of the hull. Based on the course of the axis, the second transformation was performed to introduce additional corrections to the initial position of the point cloud. The aim of this operation was to transform the point cloud to achieve coincidence between

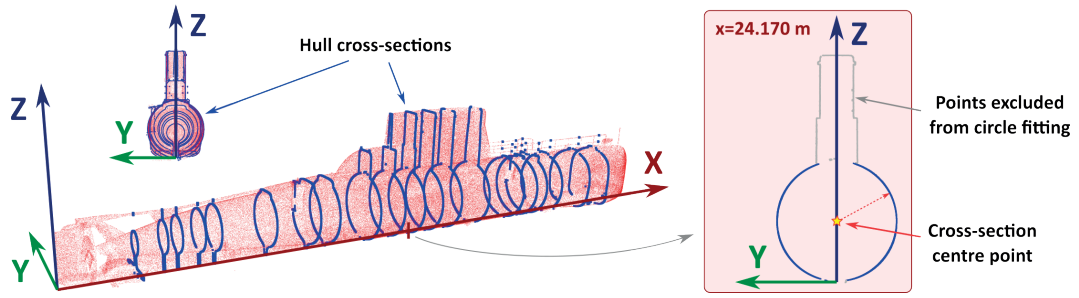


Fig. 3. Cross-sections of the YZ-plane point cloud with an example illustrating the estimation of the centre point

the axis of symmetry of the ship's hull and the X-axis of the coordinate system. The set of points in the Euclidean three-dimensional space  $\mathcal{R}^3$  was fitted using the PCA method, with a line  $\ell$  represented by a point  $M$  on the line and a direction vector  $v_\ell$ . Then, in a similar way to the keel axis, the parameter  $t$  was determined for the point on the axis at the origin of the coordinate system. Starting from the vector equation of a line in Eq. (2), the value of the parameter  $t$  for the zero value of the  $x$  coordinate is obtained from the relationship:

$$t = -x_M/x_{v_\ell}. \quad (5)$$

In a similar way to the initial transformation, the final transformation of the point cloud is a two-stage process. In the first step, there is a translation by the vector  $T_1 = -(M + T \cdot v_\ell)$ , and then a rotation by the matrix:

$$R_1 = R_Y(-\text{asin}(|x_{v_\ell}|/|v_\ell|)) R_Z(-\text{atan2}(y_{v_\ell}, x_{v_\ell})) \quad (6)$$

where  $R_Y$  and  $R_Z$  denote the elementary rotation matrices around the Y- and Z-axes of the coordinate system, respectively. The final transformation of the point cloud is given by the equation:

$$P'' = R_1(P' + T_1) \quad (7)$$

The pre-processing calculations can be summarised as follows. The original point cloud with undefined orientation

was firstly coarsely aligned to the X-axis of the coordinate system (Fig. 2). The matrix used in the second transformation was derived from the course of the axis of symmetry estimated from the set of cross-sections of the hull (Fig. 3). The resulting point cloud met the condition of coincidence between the submarine's axis of symmetry and the X-axis, which is obligatory for obtaining the expansion using the PCSE method.

#### APPLICATION OF PCSE

The standard formulae for the cylindrical projection of a point cloud using the PCSE method (see e.g. [25]) take the following form after modifications related to the horizontal orientation of the examined object:

$$P_{PCSE} = \begin{bmatrix} x_{PCSE} \\ y_{PCSE} \\ z_{PCSE} \end{bmatrix} = \begin{cases} R(\text{atan2}(z_{p^*}, y_{p^*}) + \pi/2) & \text{if } R(\text{atan2}(z_{p^*}, y_{p^*})) > -\pi/2 \\ R(\text{atan2}(z_{p^*}, y_{p^*}) + 5\pi/2) & \text{if } R(\text{atan2}(z_{p^*}, y_{p^*})) \leq -\pi/2 \\ x_{p^*} \\ \sqrt{y_{p^*}^2 + z_{p^*}^2} \end{cases} \quad (8)$$

where  $R$  is the radius of the reference cylinder. The length of the cylinder radius is determined based on the dimensions of the object. In this case, the radius corresponds to the circular cross-section of the hull (see Fig. 3). The conditions used in the calculation of the  $x_{PCSE}$  coordinate ensure symmetrical representations of the port and starboard sides relative to the YZ plane in the expansion (right panel of Fig. 4).

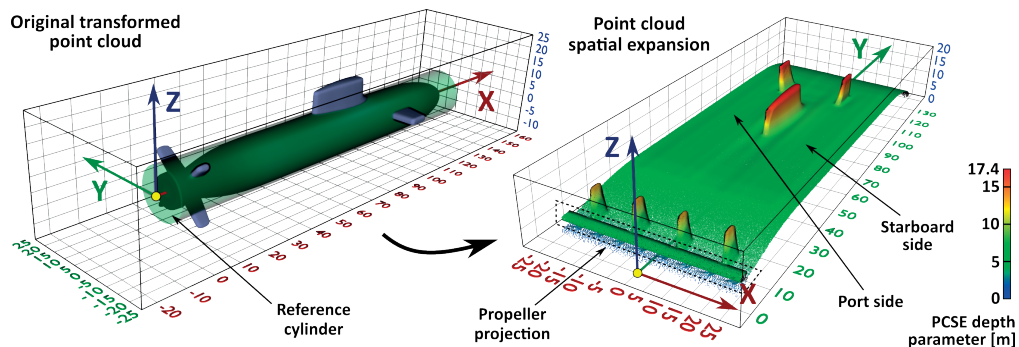


Fig. 4. Point cloud spatial expansion of a sample submarine model

The transformation defined by the PCSE method creates an alternative point cloud coordinate system. The curvilinear shape of the ship is presented by the expansion in relation to the reference cylinder with radius  $R$ , which implies that different parts of the hull are projected at different distances from the axis ( $z_{PCSE}$  coordinate). The  $y_{PCSE}$  coordinate represents the curvilinear distance of the sample point on the lateral of the cylinder from the XY-plane of the original coordinate system, which is related to the directional angle in the YZ-plane (left panel of Fig. 4). The introduction of the vertical symmetry plane of the ship in the YZ-plane of the PCSE expansion enables assessment of the hull symmetry. The  $y_{PCSE}$  coordinate corresponds to the longitudinal X-axis in the original point cloud. The third coordinate  $z_{PCSE}$  is a depth parameter in PCSE that assigns to each point an orthogonal distance relative to the estimated axis of symmetry of the ship.

It should be noted that two of the three new coordinates are geometric parameters that are not directly available in the original point cloud. The relationship between the PCSE coordinates and the axis of symmetry enhances the possibilities of inferring the shape and deformation of a symmetrical object compared to standard computational methods such as the Hausdorff distance, which is commonly used in cloud-to-cloud comparisons. Replacement of the cylindrical model of the hull with a quasi-planar PCSE representation enables local 2D plane fitting, which is particularly applicable to deformation analyses.

## DEFORMATION PARAMETERISATION

Parameterisation of the hull shape using PCSE has three important applications:

- Comparison of the surface symmetry of both sides of the ship,
- Determination of the local deformation vectors using opposite hull cross-sections (bi-symmetry),
- Validation against technical data for the ship.

The advantage of the proposed solution is that it enables us to perform analyses even in the absence of design documentation for the ship. The distribution of the relative (lack of design data) or absolute (availability of technical design) deformations calculated using PCSE means that the locations of bends and twists in the ship's hull can be determined. The mathematical model for this particular analysis is presented in the results section below.

## HULL DEFORMATION ANALYSIS

### SUBMARINE AXIS ESTIMATION AND PCSE

The initial transformation was performed using Eq. (4), which aligned the original registered point cloud with the direction of the X-axis (Fig. 2). The final fitting procedure for the ship's axis was performed using PCA based on the centres of 20 cross-sections of the hull's point cloud (Fig. 3). The means and standard deviations of the residuals in the Y- and Z-axis directions were  $1.9 \pm 5.1$  mm and  $1.6 \pm 4.0$  mm, respectively. The estimation result was verified with a T-test based on the  $\chi^2$  distribution with confidence level  $n_T$  defined by the number of centre points used in the estimation and the degree of freedom necessary to define a line in R3 [26]. The value of 35.6 obtained from the T-test met the criteria for  $n_T = 18$ , and the confidence level  $\alpha_T = 0.005$ . Then, based on the parameters of the 3D line equation, the final transformation of the point cloud was performed using Eq. (7). The spatial expansion of the point cloud of the Kobben-class ship is shown in four views in Fig. 5.

The features of the PCSE expansion dataset enable analyses of deformation to be carried that are unavailable with the original dataset. The elongated quasi-planar form of the submarine hull includes important spatial information defined by the PCSE depth parameter, which is included in the new methodology for assessing deformations.

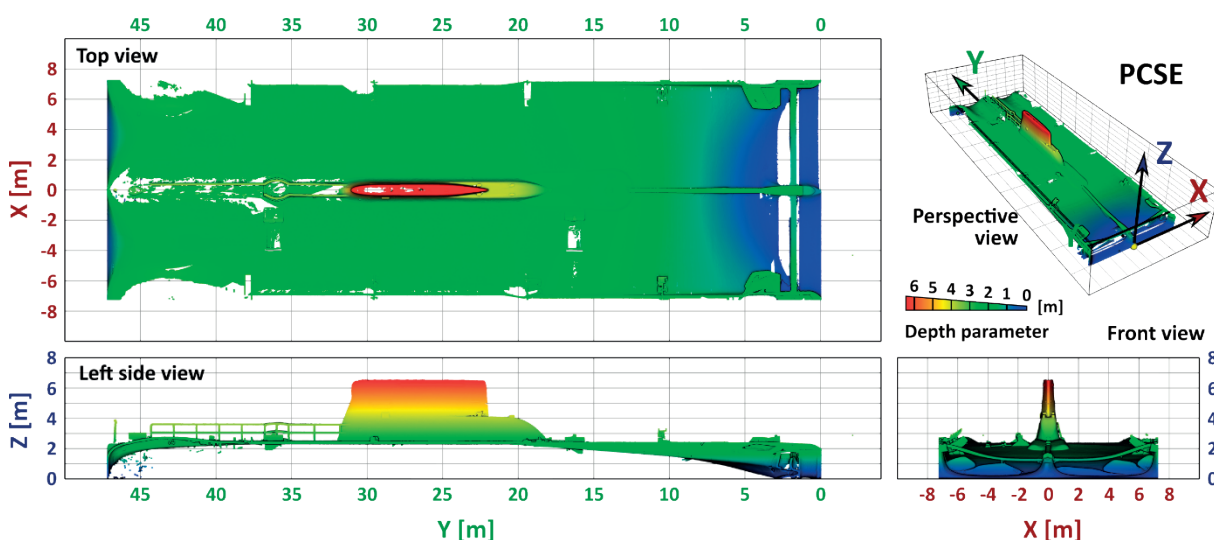


Fig. 5. Point cloud expansion for the Kobben-class submarine



## HULL SYMMETRY ANALYSIS

A surface comparison of the two sides of the ship was carried out based on the theoretical symmetry of the structure with respect to the YZ-plane. A regular square grid with a side of 0.5 m was introduced to assess the hull symmetry. The parts of the point cloud representing the two entrances cut in the hull (cf. right panel of Fig. 1), the propeller, and the four supports of the ship were excluded from the analysis. The symmetry feature present in the PCSE expansion introduces the assignment of corresponding points through opposite values of the  $x_{PCSE}$  coordinate. Taking into account the random errors in the TLS measurements, the depth parameter estimation procedure ( $z_{PCSE}$ ) was used.

To maximise the scope of analysis using point cloud data, the variation in the point cloud resolution must be considered. A comparison of two point cloud datasets involves the problem of the different locations of the points measured by the laser scanners. In the cloud-to-cloud approach implemented in engineering software, the distances between the adjacent points from two datasets are computed, meaning that in most cases, the calculated value does not represent the topology of the two surfaces represented by the point cloud. The methodology developed here uses PCSE expansion features and introduces the local fitting of planes to the defined surroundings of the analysed point. In this case, instead of using a single point, a larger set representing the surface is used in the calculation to determine the magnitude of the displacement. This approach significantly reduces the issue of variable resolution of the point cloud in deformation analyses.

In the first stage of calculation, points with a 2.5 cm buffer were selected for each grid point. This buffer value was determined to take into account the resolution of the ship's point cloud. The transformation of the cylindrical hull surface into the expanded form in Eq. (8) allows for the determination of normal vectors after mitigation of the factor of the hull's cylindrical curvature. The eigenvectors corresponding to the three coordinates in PCSE along with variances and  $\mathbf{P}_{PCA}$  points belonging to the estimated plane were determined for the obtained sets of points with a given buffer.

Replacement of the original cylindrical discrete representation of the hull surface with an expansion significantly reduces the value of one of the variances and identifies the local normal vector  $\mathbf{V}_N$ . The estimated height parameter  $\hat{\delta}$  for a given grid point and buffer was determined from the following relationship:

$$\hat{\delta} = (d - ax_{V_N} - by_{V_N})/c \quad (9)$$

where  $a, b, c$  denote the coordinates of the unit vector  $\mathbf{V}_N$ , and  $d = \mathbf{V}_N \cdot \mathbf{P}_{PCA}$ .

When the procedure described above is applied to both sides of the ship, the result is an estimate of the PCSE depth parameter for the given grid. A comparison of the  $\hat{\delta}$  parameter was carried out taking into account the symmetry of the hull in relation to the YZ-plane. A set of additional attributes in the form of the variance in the normal vectors for the port side ( $\mathbf{V}_{PS}$ ) and starboard side ( $\mathbf{V}_{SS}$ ) and the angle between these vectors were determined as follows:

$$\gamma = \angle(\dot{\mathbf{V}}_{PS}, \mathbf{V}_{SS}) \quad (10)$$

where  $\dot{\mathbf{V}}_{PS} = \mathbf{V}_{PS} \cdot [-1 \ 1 \ 1]^T$  denotes the vector symmetric to  $\mathbf{V}_{PS}$  with respect to the YZ-plane of the PCSE expansion. The values given above are a discrete representation of the asymmetry of the ship's hull (Fig. 6).

This analysis indicates that the ship's hull is bent in the longitudinal direction, as indicated by the opposite values of the indicator  $d\hat{\delta}$  as it changes along the submarine. It should be noted that the asymmetry analysis compares the shapes of the two sides by relating the PCSE depth parameter of points located on the port side to the points on the starboard side of the ship. In this case, the central part of the hull (blue dashed polygon) had negative values of the  $d\hat{\delta}$  parameter, while the bow and stern parts (red dashed polygons) had positive values. This means that the hull, with a total length of approximately 47 m, has a Menger curvature of  $3.13E-04 \text{ m}^{-1}$ . The calculated deviations showed that 43.1% of 1029 tested hull locations had

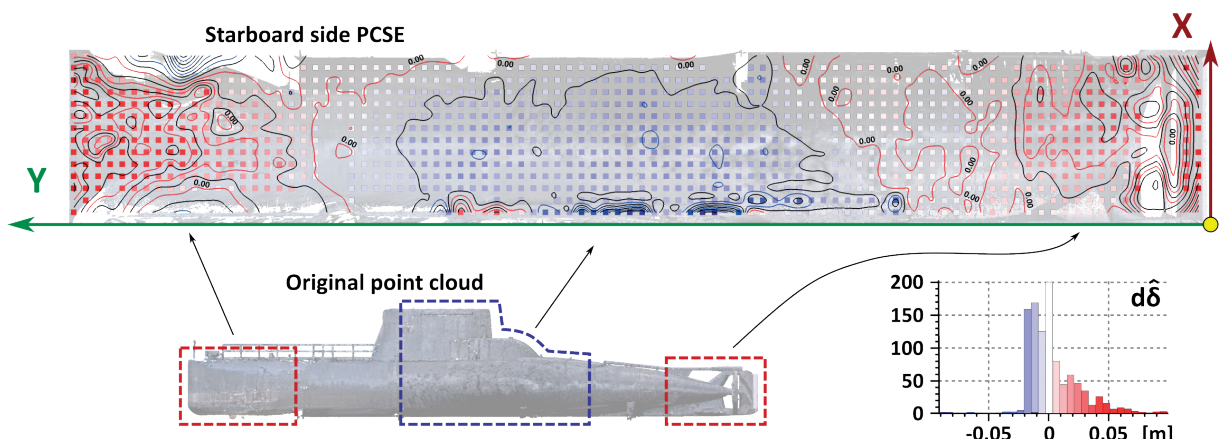


Fig. 6. Asymmetry indicators for the ship's hull



a side-to-side asymmetry  $d\delta$  not exceeding 0.01 m. Similarly, for deviations of 0.02 m and 0.05 m, the percentage values for the analysed sample were 79.6% and 95.5%, respectively.

### ANALYSIS OF OPPOSING LONGITUDINAL SECTIONS OF THE HULL

The aim of this analysis was to assess the symmetry based on the opposing sections of the hull point cloud. Longitudinal cross-sections were generated with an angular interval of 15° in half-planes perpendicular to the YZ plane of the original point cloud (left panel of Fig. 4). The cross-sections were 2 mm wide and represented the curvature of the hull along the entire length of the ship. The alternating arrangement of half-planes and cross-sections enabled a comparison of the regularity of the ship's structure both in places with a cylindrical cross-section and in cross-sections with more complex geometry. The location of the cross-sections in the original point cloud and the PCSE expansion are shown in Fig. 7.

In the expansion, opposing cross-sections were spaced at intervals of metres, and apart from one exceptional case, represented fragments of the hull with different local curvatures. The corresponding cross-sections are shown in Fig. 8. The direction angle in the YZ-plane with the 15° interval is measured clockwise from the top vertical half-plane.

Assessment of the cross-sections in two vertically placed half-planes was not possible due to a lack of data describing the bottom of the ship's keel. The different curvature of the hull in both opposing sections implied the need to modify the symmetry assessment methodology adopted previously.

Apart from the exceptional case of cross-sections in the horizontal plane (with directional angles of 90° and -90°), the opposing cross-sections differed in terms of local curvatures. This partial shape incomparability translated into different values of the PCSE depth parameter in two sections for the same coordinate value. This problem did not apply to the cylindrical parts of the hull, where the depth parameter values were similar and comparable. The two opposing cross-sections differed in places where the hull shape deviated from a circular cross-section. Fig. 9 shows four longitudinal sections with different geometries. The middle part of the graph (green) corresponds to the cylindrical part of the hull, and the bow and stern parts (red) indicate the variability in the shape of the cross-sections.

It should be noted that the same relationship of opposing cross-sections occurred for two other cross-sections placed symmetrically with respect to the XZ-plane of the original point cloud (Fig. 4). Taking into account these two relationships, the bi-symmetry of the cross-sections was introduced into the analysis. The first aspect of this

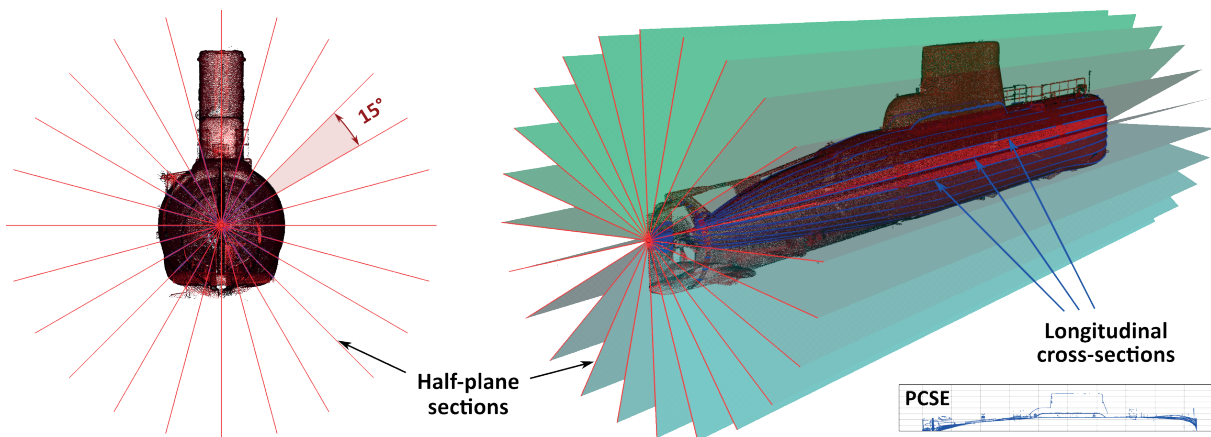


Fig. 7. Longitudinal cross-sections in regular half-planes reverse-transformed from the PCSE to the point cloud

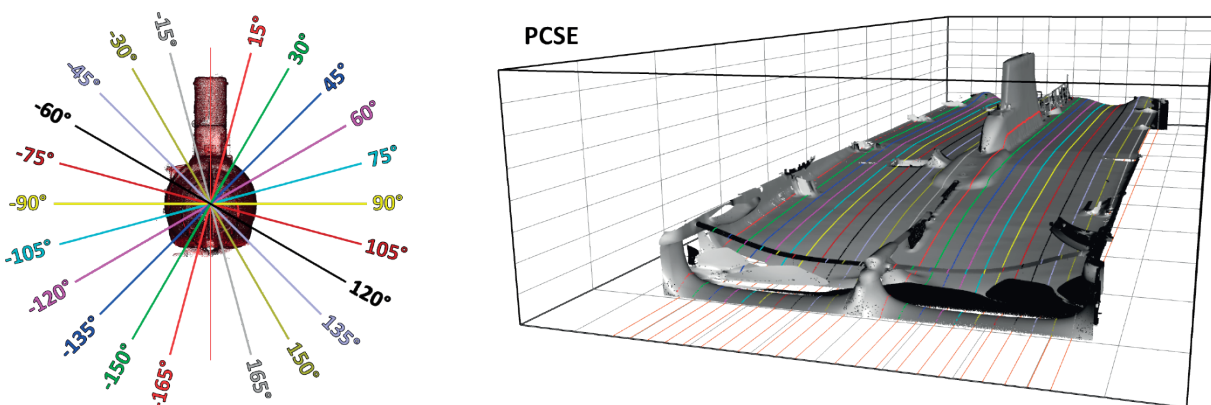


Fig. 8. Opposite assignment of longitudinal hull cross-sections



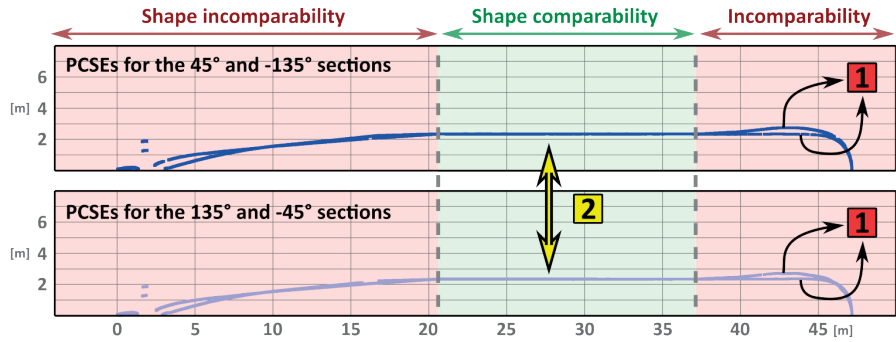
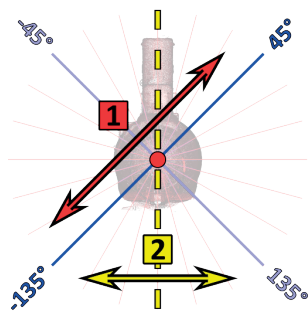


Fig. 9. Principle of double symmetry for the longitudinal sections

bi-symmetry was the correspondence of cross-sections in half-planes located opposite the estimated PCSE expansion axis (Figs. 7 and 8). This aspect is represented in Fig. 9 by a red arrow and the number “1” in a red square. The second aspect resulted from the analogous relationship of two other symmetrically located cross-sections, which are marked with a yellow arrow and the number “2” in a yellow square. The combination of data from these four corresponding cross-sections enabled the introduction of a second method of parameterising the symmetry of the ship.

Opposing longitudinal sections were selected according to the relationship:

$$S^i \sim S^{i-180^\circ} \quad \text{where } i \in \{15^\circ, 30^\circ, \dots, 90^\circ\} \quad (11)$$

When determining the value of the depth parameter along the profile, we took into account the random errors occurring in TLS measurements and the different degrees of coverage of the cross-sections with points from the cloud. The methodology adopted here included fitting lines into sets of points  $\mathcal{K}^{(y)}$  created in the vicinity of  $y_{PCSE}$  coordinates counted with a specific interval. The central values of the sets  $\in(0, 0.2, \dots, 47.0)$  were selected according to the dimensions of the submarine. Points forming the cross-section ( $P_{PCSE}$ ) were included in the set  $\mathcal{K}$  if they were located in the buffer with a radius  $\varepsilon$  of 0.05 m:

$$\mathcal{K}^{(y)} \xrightarrow{fit} l(y) \quad \text{where } (P_{PCSE} \in \mathcal{K}^{(y)} \text{ if } |y_p - y| < \varepsilon) \quad (12)$$

The estimated  $i$ -th point of the cross-section in the given set  $\mathcal{K}^{(y)}$  was calculated for the central value  $y$  on the fitted line  $l(y)$  and gave the coordinates  $\hat{P}_i^{(y)} = [y \quad l(y)]^T$ . As a result, a regular grid of points was obtained along

the longitudinal sections  $S$ , spaced 0.2 m apart along the  $Y$ -axis. The completeness of the point sequence depended on the availability of points measured by the scanner in the cross-section. The regularity of the distribution of points on the cross-sections enabled us to assess the bi-symmetry of corresponding opposing cross-sections (see Fig. 9). The values of submarine hull deflections obtained based on the bi-symmetry criterion are shown in Fig. 10.

The parameter variability is only presented for the starboard side, as the second stage of the analysis (see Fig. 9) introduces the factor of symmetry with respect to the  $YZ$ -plane of the spatial expansion. The greatest differences in the value of the depth parameter again occurred at the bow and stern of the submarine. The mean and standard deviation for the full sample were 2.8 cm and 3.5 cm, respectively; however, when the extreme values at the bow and stern for  $Y \in (3m; 46m)$  were excluded, these values decreased to 2.3 cm and 1.9 cm. Differences in the depth parameter of close to zero (blue) indicate longitudinal bending of the axis, which was fitted to the hull cross-sections (see Fig. 3).

## NORMAL VECTOR FIELD ANALYSIS

The depth parameter expresses the topology of the surface points (the submarine's hull) and its symmetry element (axis). The distribution of normal vectors in the original point cloud is characterised by an orientation orthogonal to the ship's axis, but is variable depending on the radial position of the point in the cross-section of the hull (see the right panel of Fig. 3 and the left panel of Fig. 8). Spatial expansion represents the shape of a symmetrical object in an alternative way, by replacing the curved surface of the object with a pseudo-planar form with a depth parameter assigned. In this case, pseudo-planarity

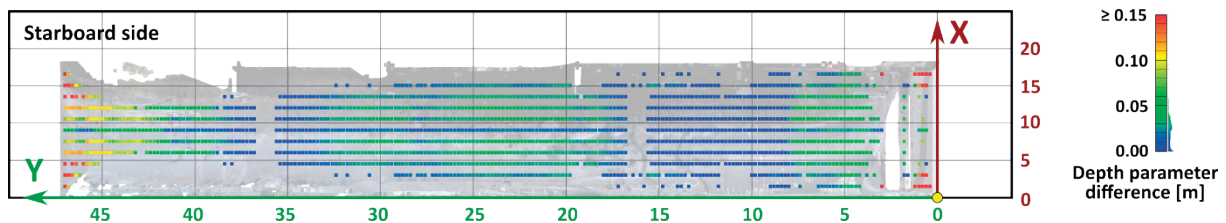


Fig. 10. Bi-symmetry of the ship's hull

means the elongated form of the dataset, which is a fully 3D model due to the use of the three-coordinate expansion of the PCSE presented in Eq. (8). Another feature of the transformation is the modification of the distribution of normal vectors, which take a common main direction when expanded by projecting the ship's symmetry axis as a plane.

A vector field analysis gives the shape variability and the location of surface deformations. In this study, we used CloudCompare software [27], which implements the curvature estimation procedure from the PCL library [28]. The curvature at each point is determined by least-squares fitting of a quadratic surface onto a small section of the point cloud in the vicinity of the analysed point. The curvature is estimated using eigenvalues of the covariance matrix of a local neighbourhood of the considered query point [29]. The results of an analysis of the curvature variability of the expanded point cloud are shown in Fig. 11.

the aft body (rear) part of the hull in the coordinate range  $y_{PCSE} \in (3m; 15m)$ , we see that significant deformations occur on the starboard side of the ship (Fig. 11). Similarly, in the parallel middle body of the hull, shape irregularities can be identified on both sides of the submarine. At the front, and especially on the starboard side, changes in curvature occur at weld joints. The largest changes in the parameter were recorded at the propeller rim projected in PCSE around the coordinate  $y_{PCSE} = 0m$ .

Next, the dependence of the vector field variability parameters (dVN, Fig. 11) and the depth parameter (dp, see Fig. 5) and the deviation of the depth parameter relative to the symmetry plane of the submarine (ddp, see Fig. 6) were examined. The correlation between the two sets of parameters is shown in Fig. 12.

In both cases, no significant correlation ( $r$ ) was obtained between the analysed variables. The reason for this is the

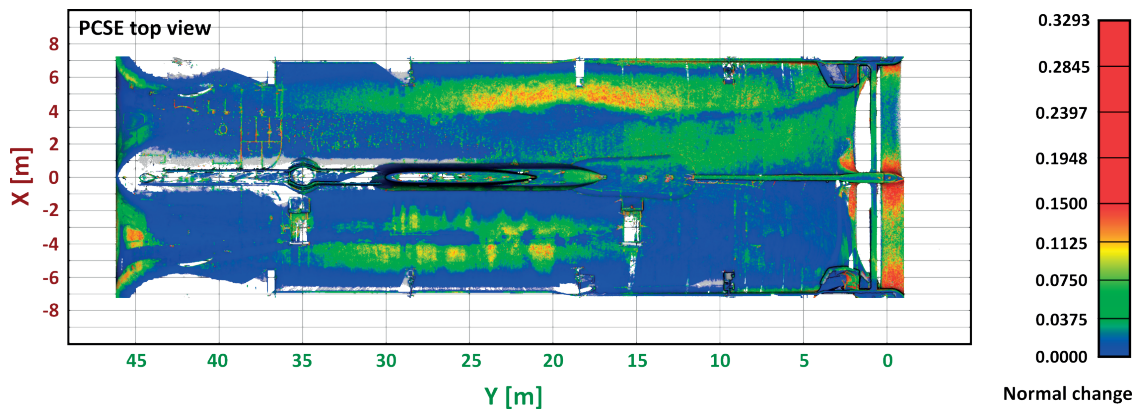


Fig. 11. Rate of change of the submarine hull's curvature

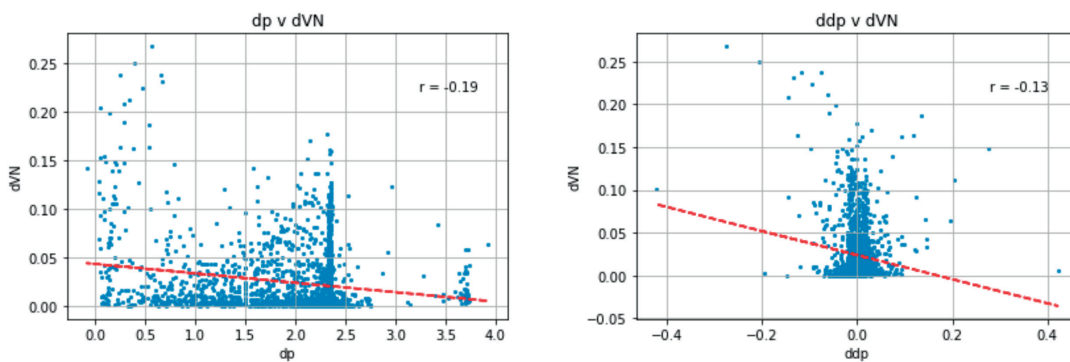


Fig. 12. Correlation between the depth parameter (left panel) and the deviation in the depth parameter (right panel) with the change in the direction of normals in PCSE

An increase in the parameter value indicates deformation of the submarine's hull. Theoretical circular cross-sections of the hull should be considered that exclude the protruding parts of the vessel, such as the tower or propeller. Zero values for the change in the direction of the normal vectors in the PCSE expansion (blue) indicate a lack of significant convexities and concavities in the hull. The results should be considered jointly with the values of the PCSE depth parameter. For

possibility of obtaining low curvature values for the fitted quadratic surfaces for different values of the PCSE depth parameter. For example, if a dent in the hull has a similar radius of curvature in its central part, the PCSE expansion will result in values of the depth parameter with a small range of variability, although these will be significantly different from the original, undeformed hull surface. In this case, a change in the direction of the normals will be noted only at the borders

of the dent, and not in its central part. Nevertheless, the mere presence of a change in the vector field is an important basis for further evaluation of the PCSE depth parameter and assessment of hull deformation.

### COMPARISON WITH DESIGN DATA

The results of the symmetry analysis (Section 3.2) and the bi-symmetry analysis (Section 3.3) provide two sources for parameterising the shape of the submarine hull. The convergence of the results from both analyses was assessed by comparison with the design data, which were transformed into the coordinate system described in Section 2.2. Information regarding the theoretical shapes of 20 sections of the ship's hull was obtained from the documentation. Next, the planar coordinates of points in the directions at intervals of 15°, in an analogous way to the bi-symmetry analysis (Fig. 8), were read for each cross-section. The procedure for obtaining design data is illustrated in Fig. 13.

In the first step of processing of the design data, the coordinates of the local axis of symmetry and the shape of the ship's hull were determined (yellow circle in the right panel of Fig. 13). In the second step, the Y- and Z-coordinates

in the cross-sectional plane were read in the given directions with the adopted angular interval. In the third step, the distance between each designated point and the symmetry axis was calculated, which created the set of reference values for the PCSE depth parameter. The coordinates of the reference markers from the original point cloud system were transformed to the spatial expansion system using Eq. (8), and then compared with the results of the two analyses of the ship hull symmetry. A comparison of the results is presented in Fig. 14.

The distributions of the differences in the depth parameter obtained from two symmetry analyses show similarities. The deviations are higher in the case of bi-symmetry, which involved a two-stage assessment of the hull shape (cf. Fig. 9). In the case of asymmetry of the ship's sides relative to the YZ-plane (Section 3.2), the average deviation compared to the design data was 2.3 mm, with a standard deviation of 11.7 mm, while the bi-symmetry analysis using opposing cross-sections was characterised by an average deviation of 12.0 mm and a standard deviation of 17.4 mm. These values indicate near-centimetre convergence of the results, which proves the validity of the proposed solution even without access to the ship's design data.

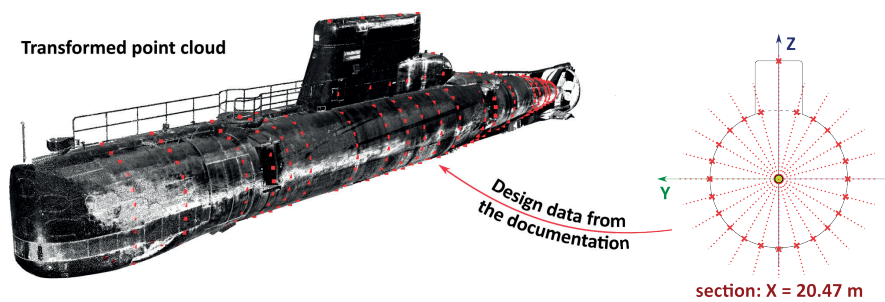


Fig. 13. Design data for the submarine hull

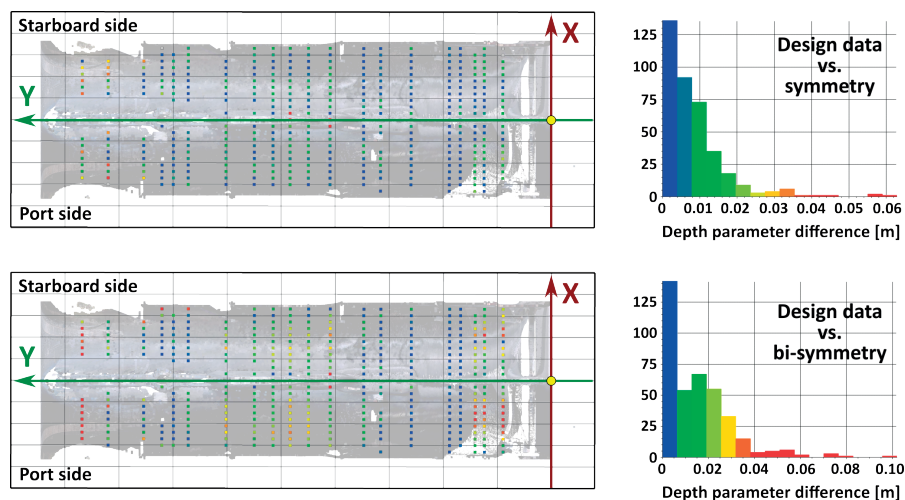


Fig. 14. Comparison of results from the analyses of design data and the hull's asymmetry (top panel) and bi-symmetry (bottom panel)

## CONCLUSION

This study has quantitatively assessed the shape and deformation of a Kobben-class submarine's hull using the PCSE method. The following results were obtained. An analysis of the hull asymmetry was conducted in two scenarios, with and without access to technical documentation. In the absence of technical documentation, the asymmetry of the hull was analyzed by comparing the port and starboard sides, as well as opposite cross-sections of the point cloud. The average asymmetry deviation was found to be 2.3 mm for two-sided symmetry and 12.0 mm for bi-symmetry. The results were verified using theoretical values derived from the design data for the Kobben-class submarine, thus demonstrating the effectiveness of the proposed method in terms of detecting deformations even without design references.

The local hull deformation was determined by examining the normal vector field in the spatial expansion of the point cloud. A statistical analysis showed no significant correlation between the changes in the normal vectors and the PCSE depth parameter (correlation coefficient  $r = 0.15$ ), indicating that a combined analysis of both metrics is necessary for a detailed deformation assessment. The curvature analysis revealed that the hull had local irregularities, particularly in the bow and stern sections. A total of 43.1% of the 1029 tested hull points showed asymmetry values ( $\delta$ ) not exceeding 0.01 m. When the threshold was increased to 0.02 m and 0.05 m, the proportions were 79.6% and 95.5%, respectively.

In the bi-symmetry analysis, the mean and standard deviation of the deformation along the entire hull were found to be 2.8 cm and 3.5 cm, respectively. When extreme values at the bow and stern were excluded, the average bi-symmetry deviations were reduced to 2.3 cm and 1.9 cm. These results confirm that the middle part of the hull had minimal deformation, while the bow and stern experienced more significant irregularities. A comparison with the ship's design data showed an average deviation of 2.3 mm for the asymmetry analysis and 12.0 mm for bi-symmetry, with standard deviations of 11.7 mm and 17.4 mm, respectively. These small deviations highlight the robustness of the PCSE method for identifying hull deformation.

In conclusion, the quantitative analysis presented here confirms that the PCSE method is effective for the detection of hull deformations in both symmetric and bi-symmetric scenarios. It can be applied even in the absence of design data, making it a valuable tool for non-destructive testing of submarine hulls during dry dock measurements. Future research should focus on incorporating the curvature variability of the ship's axis to improve the accuracy and scope of hull deformation analysis.

## ACKNOWLEDGEMENTS

The authors thank the Rector-Commandant of the Polish Naval Academy of the Heroes of the Westerplatte for providing access to the Kobben-class submarine for measurements and use in this research.

The Python code package with the implementation of the study methodology is available from the ZENODO repository under doi: 10.5281/zenodo.13948394.

## REFERENCES

1. Kiciński R, Szturomski B, Świątek K. Analysis of the possibility of a submarine implosion using finite element method. *Journal of Physics: Conference Series*, IOP Publishing, vol. 2130, 012006, 2021. <https://doi.org/10.1088/1742-6596/2130/1/012006>.
2. Eisenmann DJ, Enyart D, Lo C, Brasche L. Review of progress in magnetic particle inspection. *AIP Conference Proceedings*, American Institute of Physics, vol. 1581, pp. 1505–1510, 2014. <https://doi.org/10.1063/1.4865001>.
3. Ali KB, Abdalla AN, Rifai D, Faraj MA. Review on system development in eddy current testing and technique for defect classification and characterization. *IET Circuits, Devices & Systems*, vol. 11, oo. 4, pp. 338-351, 2017. <https://doi.org/10.1049/iet-cds.2016.0327>.
4. Honarvar F, Varvani-Farahani A. A review of ultrasonic testing applications in additive manufacturing: Defect evaluation, material characterization, and process control. *Ultrasonics*, vol. 108, 106227, 2020. <https://doi.org/10.1016/j.ultras.2020.106227>.
5. Ren L, Li HN, Sun L, Li DS. Development of tube-packaged FBG strain sensor and application in the vibration experiment of submarine pipeline model. *Advanced Sensor Technologies for Nondestructive Evaluation and Structural Health Monitoring*, SPIE, vol 5770, 2005. <https://doi.org/10.1117/12.597596>.
6. Basu R, Simonsen BC, Egorov GV, Hung CF, Lindstrom P, Samuelides E, ..., Yoshikawa T. ISSC Committee V.1: Damage Assessment After Accidental Events, 17th International Ship And Offshore Structures Congress, 16-21 August 2009, Seoul, Korea, vol. 2, 2009, (Accessed on-line: <https://www.issc2022.org/wp-content/uploads/DAMAGE-ASSESSMENT-AFTER-ACCIDENTAL-EVENTS.pdf>).
7. Ziha K. Displacement of a deflected ship hull. *Marine Technology and SNAME News*, vol. 39, no. 01, pp. 54–61, 2002. <https://doi.org/10.5957/mt1.2002.39.1.54>.
8. Stambaugh KA, Wood WA. Ship fracture mechanisms investigation (No. SSC-337/PT. 1), 1990, Ship Structure Committee, U.S. Coast Guard (G-MTH), Washington D.C., USA.
9. Yao Y, Yang Y, He Z, Wang Y. Experimental study on generalized constitutive model of hull structural plate with multi-parameter pitting corrosion. *Ocean Engineering*,

vol. 170, pp. 407-415, 2018. <https://doi.org/10.1016/j.oceaneng.2018.10.038>.

10. Kiddy JS, Baldwin CS, Salter TJ. Hydrostatic testing of a manned underwater vehicle using fiber optic sensors. In Proceedings of OCEANS 2005 MTS/IEEE, vol. 2, pp. 1876-1881, 2005. <https://doi.org/10.1109/OCEANS.2005.1640031>.
11. Kenno SY, Das S, Kennedy JB, Rogge RB, Gharghour M. Residual stress distributions in ship hull specimens. Marine structures, vol. 23, no. 3, pp. 263-273, 2010. <https://doi.org/10.1016/j.marstruc.2010.07.001>.
12. Moon D, Chung S, Kwon S, Seo J, Shin J. Comparison and utilization of point cloud generated from photogrammetry and laser scanning: 3D world model for smart heavy equipment planning. Automation in Construction, vol. 98, pp. 322-331, 2019. <https://doi.org/10.1016/j.autcon.2018.07.020>.
13. Vosselman G, Maas HG. Airborne and terrestrial laser scanning. CRC Press Taylor & Francis, Whittles Publishing, Caithness, Scotland, UK, 2010.
14. Huang X, Mei G, Zhang J, Abbas R. A comprehensive survey on point cloud registration. arXiv 2021. <https://doi.org/10.48550/arXiv.2103.02690>.
15. Wakisaka E, Moribe Y, Kanai S. TLS point cloud registration based on ICP algorithm using point quality. International Archives of the Photogrammetry, Remote Sensing and Spatial Information Sciences, vol. XLII-2/W13, pp. 963-968, 2019. <https://doi.org/10.5194/isprs-archives-XLII-2-W13-963-2019>.
16. Roynard X, Deschaud JE, Goulette F. Paris-Lille-3D: A large and high-quality ground-truth urban point cloud dataset for automatic segmentation and classification. International Journal of Robotics Research, vol. 37, no. 6, pp. 545-557, 2018. <https://doi.org/10.1177/0278364918767506>.
17. Stjepandić J, Bondar S, Korol W. Object recognition findings in a built environment. In: DigiTwin: An Approach for Production Process Optimization in a Built Environment, 2022, Springer Cham, Switzerland. [https://doi.org/10.1007/978-3-030-77539-1\\_8](https://doi.org/10.1007/978-3-030-77539-1_8).
18. Huang Z, Wen Y, Wang Z, Ren J, Jia K. Surface reconstruction from point clouds: A survey and a benchmark. arXiv preprint arXiv:2205.02413, vol. 46, no. 12, pp. 9727-9748, 2022. <https://doi.org/10.1109/TPAMI.2024.3429209>.
19. Sundaresan P, Antonova R, Bohgl J. Diffcloud: Real-to-sim from point clouds with differentiable simulation and rendering of deformable objects. 2022 IEEE/RSJ International Conference on Intelligent Robots and Systems (IROS), IEEE, pp. 10828-10835, 2022. <https://doi.org/10.1109/IROS47612.2022.9981101>.
20. Zhu L, Chen Z, Wang B, Tian G, Ji L. SFSS-Net: Shape-aware filter and semantic-ranked sampler for voxel-based 3D object detection. Neural Computing and Applications, vol. 35, pp. 13417-13431, 2023. <https://doi.org/10.1007/s00521-023-08382-7>.
21. Dabrowski PS. Novel PCSE-based approach of inclined structures geometry analysis on the example of the Leaning Tower of Pisa. Measurement, vol. 189, 110462, 2022. <https://doi.org/10.1016/j.measurement.2021.110462>.
22. Dabrowski PS, Zienkiewicz MH, Truong-Hong L, Lindenbergh R. Assessing historical church tower asymmetry using point cloud spatial expansion. Journal of Building Engineering, vol. 75, 107040, 2023. <https://doi.org/10.1016/j.jobbe.2023.107040>.
23. Wiśniewski Z, Zienkiewicz MH. Empirical analyses of robustness of the square Msplit estimation. Journal of Applied Geodesy, vol. 15, no. 2, pp. 87-104, 2021. <https://doi.org/10.1515/jag-2020-0009>.
24. Snow K, Schaffrin B. Line fitting in Euclidean 3D space. Studia Geophysica Et Geodaetica, vol. 60, pp. 210-227, 2016. <https://doi.org/10.1007/s11200-015-0246-x>.
25. Dabrowski PS, Specht C. Spatial expansion of the symmetrical objects point clouds to the lateral surface of the cylinder—Mathematical model. Measurement, vol. 134, pp. 40-47, 2019. <https://doi.org/10.1016/j.measurement.2018.10.036>.
26. Tiberius CC, van der Marel H, Reudink RHC, van Leijen FJ. Surveying and mapping. TU Delft Open, Delft University of Technology, The Netherlands, 2021.
27. Girardeau-Montaut D. CloudCompare. France: EDF R&D Telecom ParisTech, 2016, (Accessed on-line: [https://www.eurosdrr.net/sites/default/files/images/inline/04-cloudcompare\\_pcp\\_2019\\_public.pdf](https://www.eurosdrr.net/sites/default/files/images/inline/04-cloudcompare_pcp_2019_public.pdf)).
28. Rusu RB, Cousins S. 3d is here: Point cloud library (pcl). In 2011 IEEE International Conference on Robotics and Automation. IEEE, pp. 1-4, 2011. <https://doi.org/10.1109/ICRA.2011.5980567>.
29. Douros I, Buxton BF. Three-dimensional surface curvature estimation using quadric surface patches. Scanning, 2002, (Accessed on-line: <https://api.semanticscholar.org/CorpusID:14748373>).